Nov 16th, 12:00 AM

Purlin Failures in the Vicinity of Lap Joints and Internal Supports

K. T. Kavanagh

PURLIN FAILURES IN THE VICINITY OF LAP JOINTS AND INTERNAL SUPPORTS

K. T. Kavanagh*

ABSTRACT

Continuous span tests of commercially produced Z and C section in 450MPA steel (65KSI) have demonstrated two characteristic modes of failure due to the presence of concentrated forces (or supports). The failure modes can be significant in terms of design stresses when the loads or supports utilise simple web connections, permitting distortion of the cross section and rotation of the compression flange. Lapped purlin systems are shown to exhibit similar failures due to the presence of concentrated bolt forces at the extremities of the lap.

Distortional failures of two types can be shown to occur; 1) a stiffened flange mode of failure due to the downward rotation of the flange adjacent to the point of loading, or 2) an unstiffened mode of failure due to upward rotation of the compression flange some distance removed from the point of loading. The latter mode can produce significant decreases in strength of the section due to geometry change and plastic deformation in the flange stiffener.

A simplified mechanical model is presented to analyse sections which lose strength due to geometry change. The model is used to predict the relatively poorer performance of purlins with curved stiffeners, and the associated poorer performance of sections with stiffeners at less than 90^{o}.

*Department of Civil Engineering
University of Western Australia
Nedlands, Western Australia

INTRODUCTION

An extensive series of tests was carried out during the years 1977 and 1978 to determine the commercial viability of two purlin systems, both fabricated from 450MPA steel (65KSI). Of the two purlin systems, the first was an upgrade from 370MPA to 450MPA, and its principal feature was the perfect point-symmetry of its cross-section. The purlin relied upon the use of gently curved stiffeners to permit press-fitting of mating sections at the purlin lap joints, which eliminated much of the handling required by typical unsymmetric lapped systems during erection. The second purlin system utilised a conventional stiffening lip, with slotted holes in the web to facilitate erection and cutting tolerances. The cross sections are shown in Fig. 1.

Continuous span tests of both cross sections produced failure patterns of the type shown in Fig. 2a and 2b. The pattern typified by Fig. 2a can be associated with any two-span continuous purlin in the absence of a lapped joint. The compression flange in 2a is rotated downward, and the failure occurs by yielding at the flange/web juncture. The failure is at a lower load than predicted by the stiffened flange provisions of both the AS1538[1] and the AISI[2] codes of practise. The pattern exhibited in Fig. 2b rotates the flange in the opposite direction, and the failure is typically found to occur 600 to 1000 mm away from points of support or from edges of laps. The failure pattern in Fig. 2b is similar to that of an unstiffened mode of failure, and is characterised by a premature yielding of the lip stiffener.

BACKGROUND

The difference between the failures shown in Fig. 2a and 2b can be explained from the simple model in Fig. 3. The mechanical model is based upon the assumptions:

1) that the tension flange is not significant in the mode of failure,
2) that the lateral purlin movement and the lateral stresses are small,
3) that the flange/web junction is an effective centre of rotation for the flange and stiffener,
4) that the deflections are small.

A mode (1) type of failure (Fig. 2a) can be shown to produce an additional compressive stress in the compression flange. The added stress results in premature failure of the compression flange due to plastic yield at the flange/web connection (note that the stiffener is relieved of compressive stress and does not yield). A mode (2) type of failure produces additional compressive stresses in the stiffener, but at the same time delays stiffened plate buckling in the flange. The additional stresses produce premature failure of the stiffener. The stress patterns are shown in Fig. 3.

Mode (2) failures can be shown to effect design allowable stresses when point loads are applied to the purlin spans. The interaction between shear and bending in the purlin can be shown to differ from both design codes, AS1538 §3.4.2.b and AISI §3.4.3 A comparison of the experimental and design code values is shown in Fig. 4 for the commercial 150mm (6in) deep purlin of Fig. 1b. It can be readily seen that there is a significant deviation from the theoretical curve when the section approaches a condition of pure moment. The non-conservative nature of the failure is significant, and represents a change in the failure pattern from a short wave length (shear/bending) to a long wave length (flange only). It is important to note that the non-conservative values do not result for all purlins, but tend to be most significant when the bending provisions of the respective codes, AS1538 §3.4.2.b or AISI §3.4.2.1, 3.4.2.2, approach the yield stress of the material (i.e. a similar trend was not observed in the corresponding 200mm (8in) deep section).

A simple test was conducted in 1980 to investigate the behaviour of the purlin cross-sections in the vicinity of lap joints. A simply supported beam was lapped at the centre, and loaded by a concentrated load at the centre of the span (see Fig. 5). The simply supported beam represents an approximation of the conditions adjacent to the support of a continuous lapped purlin system. The test is both inexpensive and simple to perform, and its results confirm the behaviour of purlins observed from the earlier large-scale tests. The advantage in this latter test (aside from cost) is the ability to determine internal forces from statics alone, as shown in Fig. 5b.

Results of the lapped purlin tests revealed that purlins were sensitive to moment gradient in the vicinity of the lap cut-off. (A standard lap is normally 15% of the span). Steep moment gradients produced failures adjacent to the lap, in modes resembling pure shear (very steep gradients) or the type (1) failure shown in Fig. 2a. (moderately steep gradients). Whenever significant moments remained away from the lap joint, failure reverted to a type (2) failure shown in Fig. 2b. Test results are shown in TABLE 1.

An explanation of the failure is reasonably straight-forward. The lap is symmetric with respect to the longitudinal axis, but the flanges are reversed (over/under) on each end of the specimen. Failure always occurs at the end where the lapped flanges separate. At this end, the lower flange is bent downwards under the action of bolt forces, adding compression to the stiffened flange. If yield is exceeded in the flange, a type (1) failure occurs. Approximately one (unstiffened) wave length away from the lap, the flange is bent upwards as in a beam on elastic foundations. The negative bending produces an upward motion of the flange, with added compression in the tip of the flange stiffener. If yield is exceeded in the stiffener, a type (2) failure occurs.

The simple nature of the failures could be explained by the simple model of Fig. 3, but the discrepency between the curved lip and the straight lip could not be quantified. To remedy this, a more complex model was derived, which could account for geometric changes in the cross-section as the purlin is progressively loaded.

BUCKLING ANALYSIS: DISTORTION MODEL

The original buckling analysis (Fig. 3) was upgraded to provide an incremental change of geometry and to incorporate the effects of in-plane yield stresses. The computer model shown in Fig. 6 was written for a finite strip solution, but coupling in the harmonics proved too time-consuming to be practicable. As an approximation, a single harmonic solution was adopted, with a characteristic buckle length that could vary with the critical buckle length of the deformed x-section. The approximations in the model are as follows:

1) the strains are small, but geometry changes are large
2) the section is under vertical bending only (i.e. restrained laterally
3) there is one point on the x-section that acts as an instantaneous centre of rotation (generally the flange/web junction)
4) the geometry varies as a single harmonic along the length
5) the geometry can be described by a series of segments along the x-section length, defined by a continuous polynomial
6) the effect of concentrated forces can be replaced by an initial eccentricity.

Derivation of the model follows a minimum potential energy development, utilising the single harmonic along the length and a polynomial across the cross section.

BACKGROUND FOR THE MODEL

The analysis is predicated on the definition of a 'distortional' warping energy caused by the movement of points in the cross section. The cross section is divided into straight segments, as shown in Fig. 6. Each segment is given a normal and transverse displacement defined by the rotation angles (ϕ_i) and by the segmental radii (R_{ij}) and (S_{ij}):

$$\begin{aligned} u_i &= S_{ij}\ \phi_j \\ w_i &= R_{ij}\ \phi_j \end{aligned} \qquad (1)$$

The warping constant is derived from the tangential displacements of each segment. Strains in the segment are determined from the (N-1) equations of compatibility and the (1) equation of equilibrium relating the segments to the total cross section. The computational steps are summarised below:

1. Compute R_{ij} and S_{ij} for segment (i):

$$\begin{aligned} R_{ij} &= S_i + S_j\cos(\alpha_i-\alpha_j) \quad \text{(sum on j=1,i-1)} \\ S_{ij} &= S_j\cos\alpha_j\sin\alpha_i - S_j\sin\alpha_j\cos\alpha_i \quad \text{(sum on j=1,i-1)} \end{aligned} \qquad (2)$$

2. Calculate the (longitudinal) bending strains in each segment due to the tangential motion, u_j:

$$\varepsilon_j = (S_j/2) \cdot S_{jk}\, \phi_k'' \qquad \text{(sum of k)} \qquad (3)$$

3. Set up the matrix equations of compatibility and equilibrium, and solve for the uniform (longitudinal) strains:

$$\begin{bmatrix} 1 & -1 & & & & \\ & 1 & -1 & & & \\ & & 1 & -1 & & \\ & & & \ddots & & \\ & & & & 1 & -1 \\ S_1 & S_2 & S_3 & \cdots & \cdots & S_n \end{bmatrix} \begin{Bmatrix} \bar{\varepsilon}_1 \\ \cdot \\ \cdot \\ \cdot \\ \cdot \\ \cdot \\ \bar{\varepsilon}_n \end{Bmatrix} = \begin{Bmatrix} \varepsilon_1 + \varepsilon_2 \\ \varepsilon_2 + \varepsilon_3 \\ \cdot \\ \cdot \\ \cdot \\ \cdot \\ \varepsilon_{n-1} + \varepsilon_n \\ 0 \end{Bmatrix} \qquad (a)$$

(4)

$$\begin{Bmatrix} \bar{\varepsilon}_1 \\ \cdot \\ \cdot \\ \cdot \\ \cdot \\ \cdot \\ \bar{\varepsilon}_n \end{Bmatrix} = \begin{bmatrix} (1+a_1) & (2+a_2) \cdots\cdots & (2+a_{n-1}) & (1+a_n) \\ & \ddots & \vdots & \vdots \\ a_1 & \cdots\cdots (1+a_{n-2}) & (2+a_{n-1}) & (1+a_n) \\ a_1 & a_2 \cdots\cdots a_{n-2} & (1+a_{n-1}) & (1+a_n) \\ a_1 & a_2 \; a_3 \cdots\cdots a_{n-1} & & a_n \end{bmatrix} \begin{Bmatrix} \varepsilon_1 \\ \cdot \\ \cdot \\ \cdot \\ \cdot \\ \cdot \\ \varepsilon_n \end{Bmatrix} \qquad (b)$$

where:

$$a_1 = -S_1/A$$

$$a_2 = -(2S_1+S_2)/A$$

$$\cdot$$
$$\cdot$$
$$\cdot$$

$$a_{n-1} = -(2S_1+2S_2+ \cdots \; 2S_{n-2}+S_{n-1})/A$$

$$a_n = -(S_1+S_2+ \cdots \; S_{n-1})/A$$

$$A = S_1+S_2+S_3+ \cdots \; S_n$$

4. Derive the 'warping' stiffnesses from the expression for the total strain energy of the distortion:

$$\bar{\varepsilon}_i = a_{ij}\varepsilon_j \quad \text{(from Eq. 4b)} \tag{a}$$

$$\varepsilon_i = S_i/2\, S_{ij}\phi''_j = \bar{S}_{ij}\phi''_j \quad \text{(from Eq. 3)} \tag{b}$$

$$\text{Strain Energy} = \tfrac{1}{2}Et \int_{\text{length}} (\varepsilon)^2 dl \tag{c}$$

$$= \tfrac{1}{2}Et \int (\varepsilon+\bar{\varepsilon})^2 dl \tag{d}$$

$$= \tfrac{1}{2}Et \quad (\varepsilon_i^2/3+\bar{\varepsilon}_i^2)S_i \quad \text{(sum on i=1,n)} \tag{e}$$

$$= \tfrac{1}{2}Et\, S_i(\bar{S}_{iL}\bar{S}_{iM}/3 + a_{ij}a_{ik}\bar{S}_{jL}\bar{S}_{jM})\phi''_L\phi''_M \tag{f}$$

$$= \tfrac{1}{2}Et\, \phi''_L\phi''_M \left[S_i(\bar{S}_{iL}\bar{S}_{iM}/3 + a_{ij}a_{ik}\bar{S}_{jL}\bar{S}_{jM})\right] \tag{g}$$

$$= \tfrac{1}{2}Et\, \phi''_L\phi''_M\, [K_{LM}] \tag{h}$$

(5)

The transverse bending energy (due to the normal displacements, w_j) can be arranged in a concise algorithm using Lagrange interpolation. The Lagrange functions produce simple expressions for the polynomial coefficients which are ideally suited to automated integration and differentiation: Denoting the transverse coordinate by (s):

$$w(s) = L_i(s) \cdot w_i \tag{a}$$

$$= L_i \cdot R_{ij}\, \phi_j \tag{b}$$

$$L_i(s) = \frac{(s-s_1)(s-s_2)\cdots(s-s_{i-1})(s-s_{i+1})\cdots(s-s_{n+1})}{(s_i-s_1)(s_i-s_2)\cdots(s_i-s_{i-1})(s_i-s_{i+1})\cdots(s_i-s_{n+1})} \tag{c}$$

$$= b_{n+1}s^n + b_n s^{n-1} + \cdots\cdots b_2 s + b_1 \tag{d}$$

(6)

where $b_1 = \sum_{k=1}^{n} s_k \quad k \neq i$

$b_2 = \sum_{k=1}^{n}\sum_{L=1}^{n} s_k s_L \quad k,L \neq i$

.
.
.

$b_{n+1} = (s_1 s_2 s_3 \cdots s_n)$

in matrix form:

$$w(s) = \langle 1\ 1\ 1\ \cdots\ 1 \rangle \begin{bmatrix} b_{11} & b_{21} & \cdots & b_{n+1,1} \\ b_{21}x & b_{22}x & & \cdot \\ \cdot & \cdot & & \cdot \\ \cdot & \cdot & & \cdot \\ \cdot & \cdot & & \cdot \\ b_{n+1}x^n & b_{n,n+1}x^n & & b_{n+1,n+1} \end{bmatrix} \begin{Bmatrix} w_1 \\ w_2 \\ \cdot \\ \cdot \\ \cdot \\ w_n \end{Bmatrix} \qquad \text{(a)} \qquad (7)$$

where $b_{ij} = b_i(s_j)$

$$= \langle 1\ 1\ \cdots\ 1 \rangle \begin{bmatrix} & & \\ & [B] & \\ & & \end{bmatrix} \begin{bmatrix} 0 & & & \\ R & & & \\ R_{21} & R_{22} & & \\ \cdot & \cdot & & \\ \cdot & \cdot & & \\ R_{n1} & R_{n2} & \cdots & R_{nn} \end{bmatrix} \begin{Bmatrix} \phi_1 \\ \cdot \\ \cdot \\ \cdot \\ \cdot \\ \phi_n \end{Bmatrix} \qquad \text{(b)}$$

$$= \langle 1\ 1\ \cdots\ 1 \rangle \begin{bmatrix} & & \\ & [Q] & \\ & & \end{bmatrix} \begin{Bmatrix} \phi_1 \\ \cdot \\ \cdot \\ \\ \phi_n \end{Bmatrix} \qquad \text{(c)}$$

The total strain energy for the cross section is comprised of the transverse bending energy and the distortional warping energy. The bending and warping components are assembled in a matrix form in terms of the rotational angles (ϕ_i):

$$U = \tfrac{1}{2} \frac{Et^3}{12(1-\nu^2)} \int_0^L \left\{ \left(\frac{d^2w}{dx^2}\right)^2 + 2\nu \left(\frac{d^2w}{dx^2}\frac{d^2w}{dy^2}\right) + \left(\frac{d^2w}{dy^2}\right)^2 + 2(1-\nu)\left(\frac{d^2w}{dxdy}\right)^2 \right\} dx + \tfrac{1}{2} EI_w (\phi'')^2 \qquad \text{(a)} \qquad (8)$$

where: $\left(\frac{d^2w}{dx}\right)^2 = \langle \phi_1 \cdots \phi_n \rangle [Q"]^T[T][Q"] \begin{Bmatrix} \phi_1 \\ \cdot \\ \cdot \\ \cdot \\ \phi_n \end{Bmatrix}$ (b)

and: $[T] = \begin{bmatrix} 1 & 1 & 1 & 1 & 1 & \cdots & 1 \\ . & & & & & & 1 \\ . & & & & & & 1 \\ 1 & 1 & 1 & 1 & \cdots & & 1 \end{bmatrix}$ (8)

$= Q"_{kL} Q"_{jM} \phi_L \phi_M$ (sum on k,j,L,M) (c)

$= q_{kL} q_{jM} x^{(k-3)} x^{(L-3)} (k-1)(k-2)(L-1)(L-2) \phi_L \phi_m$ (d)

and: q_{kL} = coeff of Q_{kL}

etc.

5. Combine the External Work and Internal Energy to form the Potential Energy of the system.

$$\text{Work} = t \int_0^L \sigma(x) \cdot \tfrac{1}{2} (dw/dy)^2 \, dx$$

P.E. = Work - Internal Strain Energy

$$= \langle \phi_1 \cdots \phi_n \rangle \begin{bmatrix} \\ [W] - [U] \\ \\ \end{bmatrix} \begin{Bmatrix} \phi_1 \\ \vdots \\ \phi_n \end{Bmatrix}$$

6. Solve the Incremental Equations.

A NOTE ON THE INCREMENTAL FORMULATION FOR A SINGLE HARMONIC

The use of a single sine wave in the buckling solution requires that the critical buckle length be determined at each increment of the solution. At long wave lengths, the variation of critical buckling stress is not sensitive to the accurate determination of length, and a minimum value determined from a quadratic fit through three points is generally acceptable. The variation of buckle stress with length, and the quadratic approximation are shown in Fig. 7.

At each increment of the analysis, the geometry is updated according to growth in initial eccentricity, assuming that the change in shape follows the mode shape of the previous increment. Plasticity is included by removing the in-plane energy component of any segment of the cross section in which the average stress exceeds the yield stress. Resultant changes to the cross-section produce changes in the buckling stress and the critical buckle length at each increment, with rapid changes occuring near failure.

A predictor-corrector algorithm is used to incorporate geometry changes in the single sine wave solution. The predictor equation is formed from previous increments in the solution:

Buckle Length:

$$L_{cr}^{(i)} = L_{cr}^{(i-2)} + \left\{ \left(L_{cr}^{(i-1)} - L_{cr}^{(i-3)} \right) \Big/ \Delta L_{13}^{(i)} \right\} \Delta L_{01}^{(i)}$$

where $\Delta L_{rs}^{(i)} = L_{cr}^{(i-r)} - L_{cr}^{(i-s)}$

The growth in the initial eccentricity is adjusted for the change in length by computing a single Fourier component of incremental changes:

$$\Delta_o^{(i)} = b_1 \delta_o^{(1)} + b_2 \delta_o^{(2)} + \cdots b_{i-1} \delta_o^{(i-1)}$$

Δ_o = total eccentricity

δ_o = incremental eccentricity

$$b_k = \frac{1}{2\pi} \int_0^{L_k} \sin \frac{\pi x}{L_{cr}^{k}} \sin \frac{\pi x}{L_{cr}^{i}} \, dx$$

Deformation is assumed to follow the path of the lowest eigenvector in each increment.

A NOTE ON THE ESTIMATE OF INITIAL DEFORMATION

The application of concentrated bolt forces at the location of a web cleat can be approximated by concentrated horizontal and vertical forces on the web and flange of the cross-section. The effect of the bolt forces is shown schematically in Fig. 8. The mechanical system can be equated to a beam on elastic supports, in which the stiffener is subjected to both positive and negative bending. In most commercial purlin systems, the negative bending (away from the point of loading) is approximately one-fifth of the intensity of the positive bending at the point of load application. Positive and negative eccentricities can be calculated from the single sine wave approximation at each point, once the magnitude of the bending stress has been determined.

The model shown in Fig. 8 can be adapted to include horizontal restraint in the case of lapped systems. Negative eccentricities, although smaller in initial magnitude, tend to be more critical due to the rapid growth of deflection near the critical buckling load. The negative stresses produce premature yield of the flange stiffener, and a subsequent rapid degradation of strength. Positive eccentricities are associated with an increase of buckling strength due to distortion, and consequently, are not subject to severe amplification near the yield stress of the section.

A NOTE ON THE DISTRIBUTION OF STRESS ALONG THE LENGTH

Flanges near lapped sections are generally subjected to stress gradients along the axis of the member. The approximate single harmonic solution assumes that the stress state is uniform, and that it is equal to the average stress over the length of the buckle. Solutions based on average stresses are acceptable when the ratio of end stresses is between 0 and 1.0, which is the case for commercial purlins when the centre of the buckle pattern is taken to be one buckle length from the lap or support.

THE SIGNIFICANCE OF FAILURES NEAR LAPS AND PURLIN SUPPORTS

Where purlins have been designed with lip stiffeners in accordance with the provisions of the Codes (1) (2) and where the webs are not deep, both type one and type two failures occur close to the yield stress of the section. For these sections, there is very little variation of failure load until the moment gradient becomes very flat. With flat, or nearly constant, moments, the upward motion and premature yield of the stiffening lip cause the characteristic 'dip' in the interaction diagram shown in Fig. 4, The results are typified by the tests of 150mm purlins in Table 1.

For deep purlins with stiffened flanges, failure occurs below the yield stress of the section, and the effect of moment gradient is more pronounced. For these sections, type one failures rarely occur. Results for these sections are typified by the tests of 200mm purlins given in Table 1.

Sections with curved stiffeners behave similarly, but the dependence of the failure on the type one failure mode is more pronounced. Sections with stiffeners similar to Fig. 1a tend to unfold and lose stiffness at a lower stress level. The progression from geometric distortion-to initial plasticity - to failure is more rapid in curved lips, and lips deviating more than 20° from the vertical tend to be unsatisfactory. A sample set of results and computer predictions are given in TABLE 2.

Computed failure modes generally agreed with the failure mode in the experiments, to a reasonable degree of accuracy. The computed buckle modes were more gradual than the modes exhibited by the specimens, with longer buckle lengths at failure. The choice of the flange/web junction as the center of rotation was inadequate. Horizontal movements of the compression flange did affect the stress distribution in the flange and this was not incorporated in the model. Additional inaccuracies were found in the prediction of elastic moments due to lateral deflections and alignment of the supports.

The presence of flange failures due to point loads at the location of cleats (web stiffeners) is most important in regions of pure, or nearly uniform moment. Such forces can be associated with lateral bracing in the case of unsymmetric sections, or with vertical loadings at intersections with secondary members. Such loads do not produce web crippling due to the presence of stiff web connections.

CONCLUSIONS

Failures in continuous span purlin systems can be attributed to the development of secondary distortional stresses when points of concentrated load coincide with regions of high moment. Purlins with shallow cross-section, where the expected failure stresses are near the yield stress of the material, exhibit the distortional failures in regions of pure, or nearly uniform, moment. Purlins with deep cross-sections, where the web bending mode of failure is significantly below the yield stress of the material, exhibit two types of distortional failures which are dependent on the moment gradient. Satisfactory agreement with experimental results can be obtained from a simplified computer model, in which both plastic yield and geometry change are included.

REFERENCES

1. AS.1538-1974 Australian Standard: SAA Cold Formed Steel Structures Code, Standards Association of Australia.

2. AISI-1980 Specification for the Design of Cold Formed Steel Structural Members, American Iron and Steel Institute, Washington, D.C.

3. K.T. Kavanagh, Failure of Cold Formed Steel Purlins Near Pts. of Concentrated Load, 7th Australasian Conference on the Mechanics of Structures & Materials, Perth. May, 1980.

4. P.C. Reynolds, Failure of Light Gauge Steel Purlins Under Combined Shear and Bending Stresses, Honours Thesis, Dept. C.E., University of Western Australia, Oct. 1979.

5. Zetlin, Lev and Winter, George, 'Unsymmetrical Bending of Beams With and Without Lateral Bracing', Proceedings, ASCE, Volume 80, 1954.

TABLE 1

Purlin Size (mm)	Span (m)	Lap (m)	Failure Stress (MPA)	Yield Stress (MPA)	Failure Type	Computed Failure Stress***
150	4.75	0.9	425*	490**	2	440
150	2.84	0.9	456	480	1	465
150	4.4	0.75	495	---	1	440
150	3.6	0.75	485	---	1	438
150	4.4	0.6	492	505	2	480
150	3.6	0.6	469	505	1	470
200	4.6	0.9	369	480	2	380
200	4.76	0.8	350	480	2	360
200	4.95	0.6	340	480	2	335
200	3.2	0.6	452	---	1	425
200	3.2	0.8	445	500	1	455
200	4.66	0.9	360	500	2	335
200	3.0	0.9	440	500	1	465

* Stresses computed at the end of the lap.
** Tensile Test results (where available).
*** Yield based on tensile test values, or 450 MPA where not available.

TABLE 2

Purlin Size	Lip Angles*	Span (m)	Lap (m)	Failure Stress (MPA)	Yield Stress (MPA)	Computed Failure Stress
200	25^{o}, 50^{o}	5.0	1.0	280	485	260
200	30^{o}, 60^{o}	5.0	1.0	320	485	320
200	35^{o}, 70^{o}	5.0	1.0	348	485	360
200	40^{o}, 80^{o}	5.0	1.0	355	485	370

*Two segment Lips (θ_1, θ_2) with $I = 1.83t^4 \sqrt{(b/t)^2 - \frac{27600}{F_y}}$

** Acute angle to flange

PURLIN SECTIONS

TYPE 1

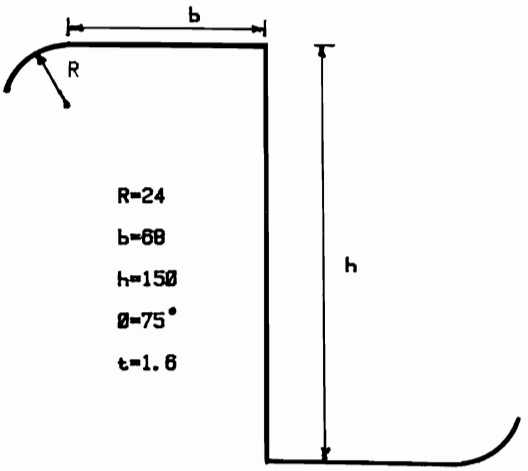

[1-a]

TYPE 2

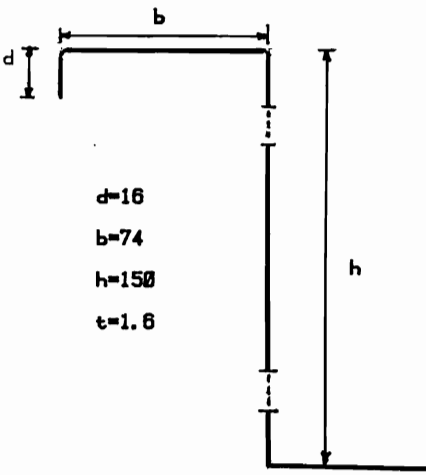

[1-b]

FIG 1

MODES OF FAILURE

TYPE 1

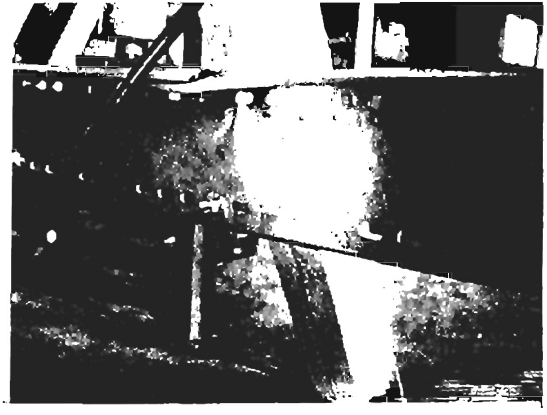

[2-a]

TYPE 2

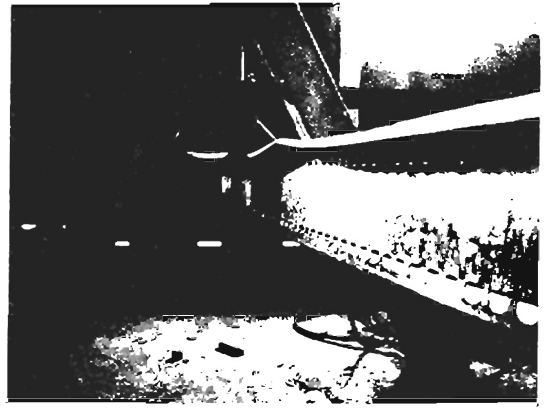

[2-b]

FIG 2

FIG 3

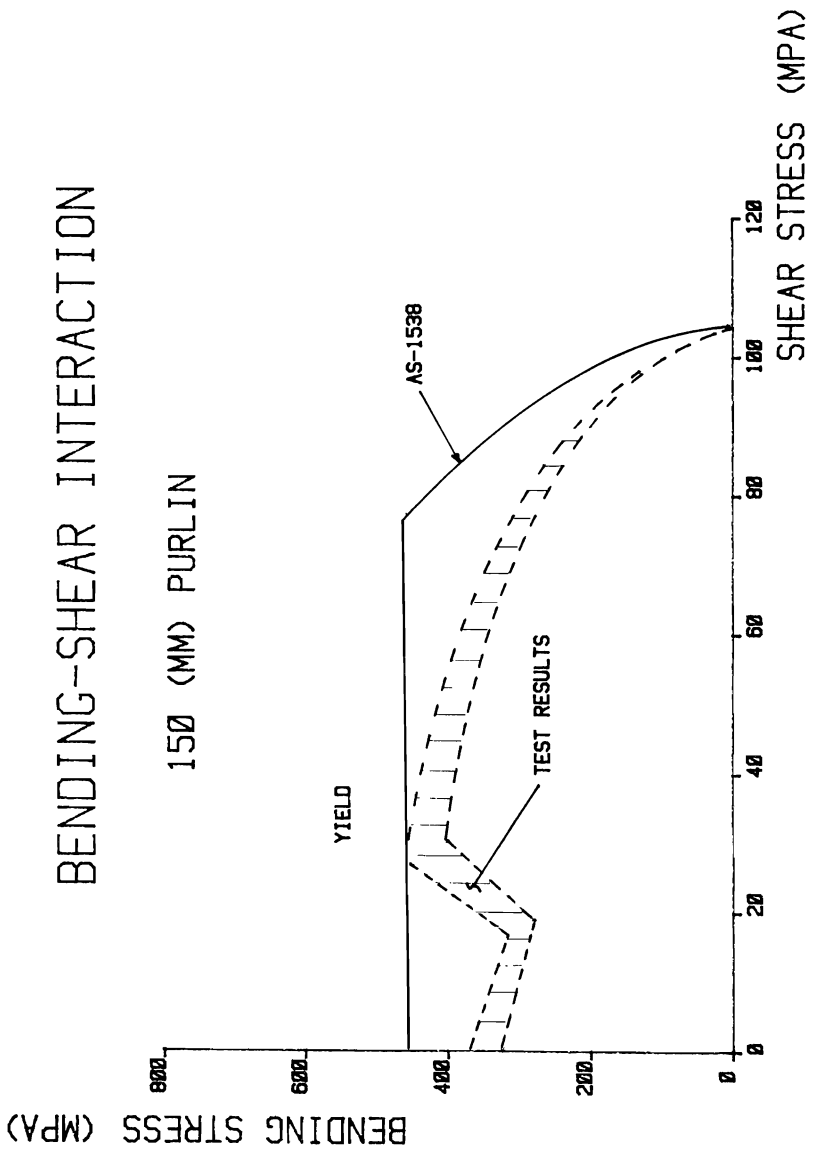
BENDING-SHEAR INTERACTION
150 (MM) PURLIN
BENDING STRESS (MPA)
SHEAR STRESS (MPA)
AS-1538
YIELD
TEST RESULTS
800
600
400
200
0
0
20
40
60
80
100
120

FIG 4

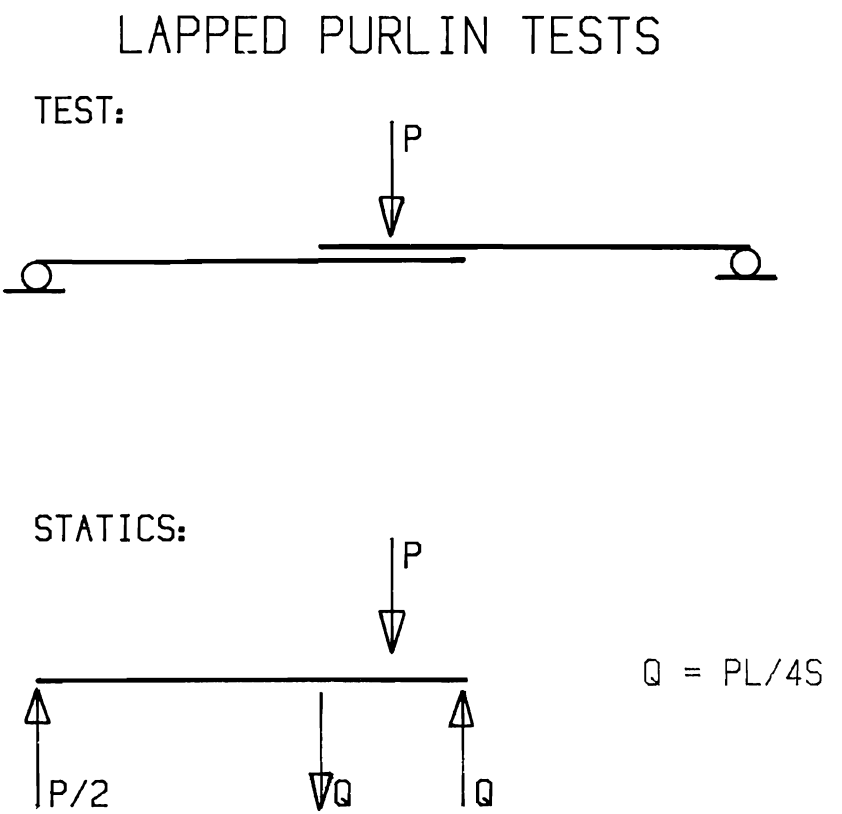

FIG 5

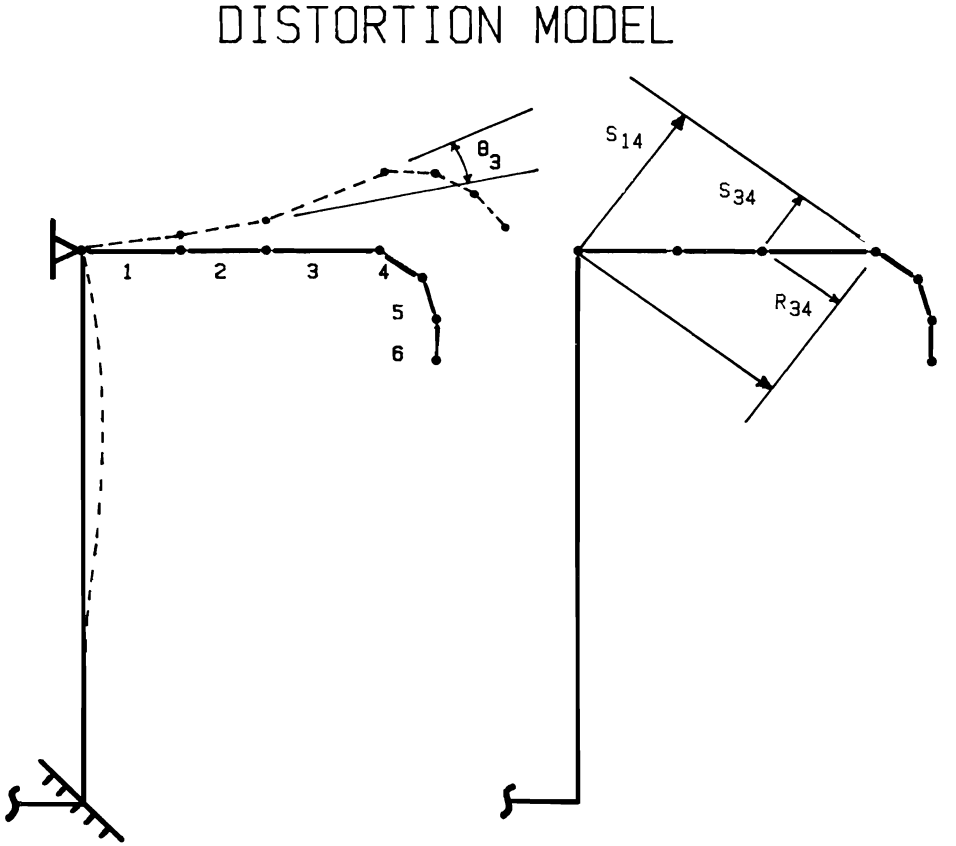

FIG 6

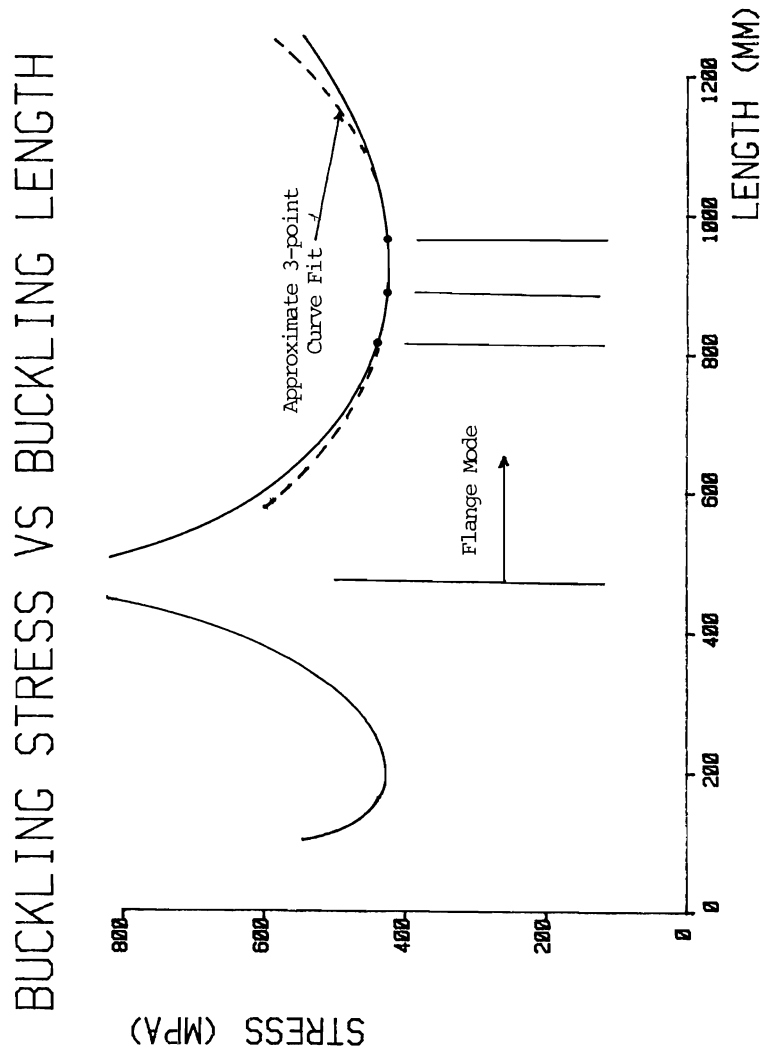
BUCKLING STRESS VS BUCKLING LENGTH
STRESS (MPA)
800
600
400
200
0
0
200
400
600
800
1000
1200
LENGTH (MM)
Approximate 3-point
Curve Fit
Flange Mode

FIG 7

CONCENTRATED BOLT FORCES

THE X-SECTION:

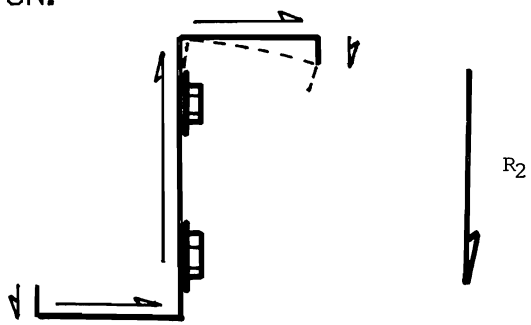

THE BEAM:

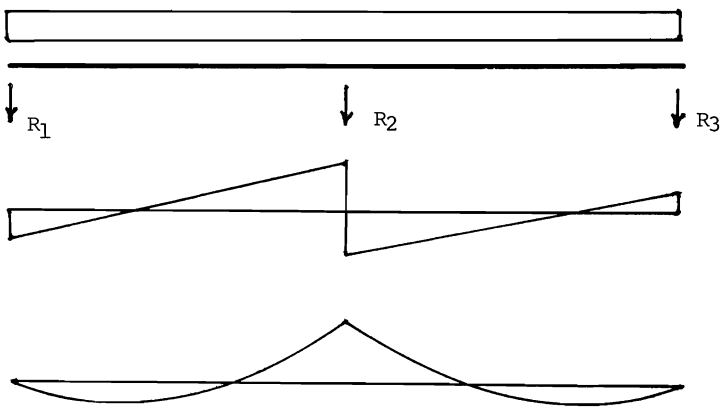

FIG 8